Available online at www.sciencedirect.com
SCIENCE DIRECT®
Journal of Solid State Chemistry 179 (2006) 1918–1923
JOURNAL OF SOLID STATE CHEMISTRY
www.elsevier.com/locate/jssc

Rapid communication

An investigation of the Nd_2O_3–MoO_3 phase system: Thermal decomposition of $Nd_2Mo_4O_{15}$ and formation of $Nd_6Mo_{10}O_{39}$

Rosemary S. Barker, Ivana Radosavljević Evans*

Department of Chemistry, University of Durham, Science Site, South Road, Durham DH1 3LE, England, UK

Received 8 February 2006; received in revised form 10 March 2006; accepted 19 March 2006
Available online 27 March 2006

Abstract

A new neodymium molybdate, $Nd_6Mo_{10}O_{39}$, has been identified in the Nd_2O_3–MoO_3 phase system. $Nd_6Mo_{10}O_{39}$ appears to be a metastable phase, which does not form directly from a stoichiometric mixture of Nd_2O_3 and MoO_3 oxides. Instead, it can be obtained by thermal decomposition of $Nd_2Mo_4O_{15}$. $Nd_2Mo_4O_{15}$ usually decomposes into $Nd_2(MoO_4)_3$, and the formation of $Nd_6Mo_{10}O_{39}$ critically depends on the heating regime used.

The structure of $Nd_6Mo_{10}O_{39}$ has been determined by single crystal X-ray diffraction. It crystallizes in the monoclinic space group $C2/c$, with unit cell parameters of $a = 12.425(1)$ Å, $b = 19.860(2)$ Å, $c = 13.882(1)$ Å, $\beta = 100.767(2)^\circ$, $V = 3365.2(5)$ Å^3 at 120 K. Nd atoms are seven and eight coordinate, and pairs of coordination polyhedra share edges and faces, respectively, to form Nd_2O_{12} and Nd_2O_{13} groups. All Mo atoms are in tetrahedral coordination environments, with some of the tetrahedra sharing corners to form pyromolybdate groups.

Keywords: Rare-earth molybdate; Crystal structure; Thermal decomposition

1. Introduction

Rare-earth molybdates display a diverse and interesting chemistry. From a structural standpoint, these phases fall into two broad categories: conventional extended inorganic structures and high nuclearity molybdenum molecular clusters. A variety of interesting and exploitable properties are exhibited by rare-earth molybdates in both structural categories. Materials in the RE_2MoO_6 family possess catalytic activity [1–3]. Compounds and solid solutions of the general formula $RE_2(MoO_4)_3$ display negative thermal expansion [4], while the Gd and Tb phases are ferroelectric and ferroelastic [5,6]. The discovery of exceptional oxide ion conductivity in $La_2Mo_2O_9$ has resulted in the preparation of numerous mixed rare-earth molybdates in this family [7]. Interesting electrical and magnetic behaviour can be found in molybdenum cluster compounds [8–10].

Two compounds having the general formula $RE_6Mo_{10}O_{39}$ (RE = Ce, Eu), with different, but related crystal structures, have been reported in the literature [11–13]. This paper presents a new neodymium molybdate, $Nd_6Mo_{10}O_{39}$, the decomposition route to its formation and its structural characterization.

2. Experimental

Preheated Nd_2O_3 and MoO_3 were mixed in a 1:4 stoichiometric ratio, thoroughly ground and fired overnight at 750 °C in an open alumina crucible. A polycrystalline product, identified as $Nd_2Mo_4O_{15}$ by powder X-ray diffraction, was formed. This powder was subsequently heated to 850 °C, slow cooled to 600 °C at a rate of 3 °C/h and then quenched to room temperature. Small pale purple crystals were isolated from the product. Their composition was found by single crystal X-ray diffraction to be $Nd_6Mo_{10}O_{39}$.

Solid state synthesis of polycrystalline $Nd_6Mo_{10}O_{39}$ was attempted by mixing Nd_2O_3 and MoO_3 in a 3:10 molar ratio, and heating the intimately ground mixture in an evacuated ampoule at 750 °C for 4 days.

*Corresponding author. Fax: +44 191 384 4737.
E-mail address: ivana.radosavljevic@durham.ac.uk (I.R. Evans).

0022-4596/$ - see front matter © 2006 Elsevier Inc. All rights reserved.
doi:10.1016/j.jssc.2006.03.023

Progress of the solid state reactions and thermal decomposition of the product were monitored by powder X-ray diffraction. Room temperature data were collected on a Bruker AXS D8 Advance diffractometer with a Solex detector. Variable temperature powder X-ray diffraction experiments were performed using a Bruker AXS D8 Advance diffractometer equipped with a Vantec detector and an Anton Paar HTK1200 high temperature stage.

Single crystal X-ray diffraction data were collected on a Bruker AXS SMART diffractometer with an APEX CCD detector, equipped with a Bede Microsource® X-ray generator, using Mo$K\alpha$ radiation. A crystal with approximate dimensions of $0.08 \times 0.08 \times 0.16\,mm^3$ was selected for data collection. A full sphere of data was collected with a frame width of 0.3° and a counting time of 20 s/frame. Data reduction was carried out using the SAINT [14] software suite. A multiscan absorption correction [15] was applied to the raw data and the resulting R_{int} was 1.4%. The crystal structure was solved by direct methods using SIR92 [16] and refined in the crystals [17] software package. A total of 250 parameters (fractional coordinates, anisotropic atomic displacement parameters, an extinction parameter and scale) were refined to the final agreement factors of $R = 1.86\%$, w$R = 2.78\%$. Full crystallographic details are given in Table 1.

Table 1
Crystallographic details for $Nd_6Mo_{10}O_{39}$

Temperature (K)	120
Crystal system	Monoclinic
Space group	$C2/c$
a (Å)	12.425(1)
b (Å)	19.860(2)
c (Å)	13.882(1)
β (deg)	100.767(2)
V (Å^3)	3365.2(5)
Z	4
Calc. ρ (g/cm^3)	4.833
μ (mm^{-1})	12.774
Total no. reflections	22568
No. unique reflections	4928
No. obs. reflections	4253
No. par. refined	250
R_{int} (%)	1.4
R (%)	1.86
wR (%)	2.78

3. Results and discussion

3.1. Decomposition of $Nd_2Mo_4O_{15}$ and formation of $Nd_6Mo_{10}O_{39}$

Europium molybdate $Eu_6Mo_{10}O_{39}$, isostructural with the title phase, was isolated in the form of single crystals from a glassy melt obtained by heating a polyoxomolybdoeuropate precursor, $[Eu_2(H_2O)_{12}Mo_8O_{27}]\cdot 6H_2O$, at 800 °C [13]. It was found that preparations were not very reproducible and the outcome depended on a number of factors, including the condition of the alumina container used, the exact composition of the starting material and the relative amounts of the precursor and seed crystals present. Attempts to prepare polycrystalline $Eu_6Mo_{10}O_{39}$ from stoichiometric amounts of Eu_2O_3 and MoO_3 by heating in evacuated quartz ampoules did not yield the desired product.

Similarly, our attempts to synthesize polycrystalline $Nd_6Mo_{10}O_{39}$ by a solid state route from a stoichiometric ratio of Nd_2O_3 and MoO_3 were not successful and $Nd_2(MoO_4)_3$ was obtained as the major phase instead.

As $Nd_6Mo_{10}O_{39}$ single crystals were first isolated from heated $Nd_2Mo_4O_{15}$, a small amount of $Nd_2Mo_4O_{15}$ from the same batch was heated to near its melting at 950 °C and quenched. The product obtained formed a solid mass at the bottom of the alumina crucible. This material was removed from the crucible and ground, and shown by powder X-ray diffraction to be single phase $Nd_6Mo_{10}O_{39}$. Fig. 1 shows the Rietveld fit to the observed powder pattern, using the structural model obtained from single crystal diffraction.

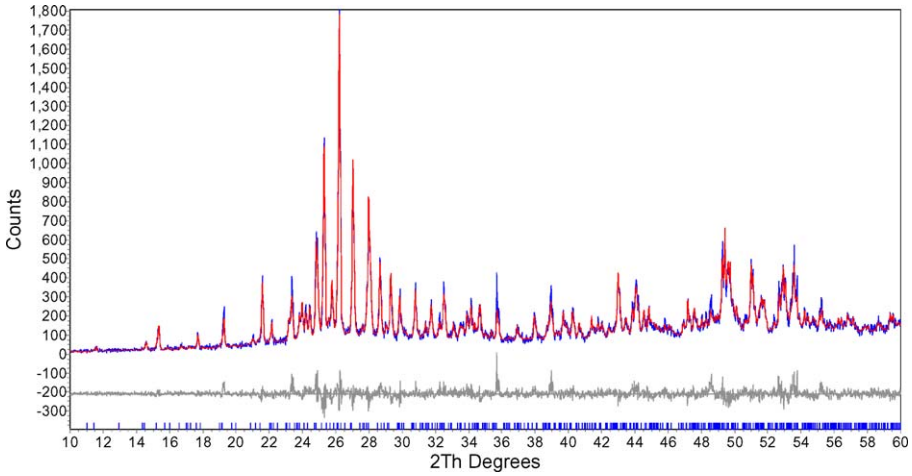

Fig. 1. Rietveld plot for $Nd_6Mo_{10}O_{39}$: the observed data (blue), calculated pattern (red) and the difference curve (grey).

In this fitting procedure, only the unit cell parameters, instrument zero point, background terms, pseudo-Voigt profile function terms and an overall isotropic temperature factor were refined.

In order to understand the formation pathway of $Nd_6Mo_{10}O_{39}$ in more detail, we also investigated the behaviour of $Nd_2Mo_4O_{15}$ as a function of temperature by in situ powder X-ray diffraction. These measurements indicate that the decomposition of $Nd_2Mo_4O_{15}$ occurs gradually at temperatures above 500 °C. Fig. 2a shows the Rietveld profile of $Nd_2Mo_4O_{15}$ (with Al_2O_3 used as an internal standard), at room temperature, while Fig. 2b shows the refinement for the sample heated in situ to 600 °C.

The new phase in the X-ray diffraction pattern at 600 °C can be identified as $Nd_2(MoO_4)_3$. Since no MoO_3 reflections are present in the pattern and thermogravimetric analysis shows a gradual mass loss above 500 °C, the decomposition of $Nd_2Mo_4O_{15}$ presumably proceeds according to the equation:

$$Nd_2Mo_4O_{15} \rightarrow Nd_2(MoO_4)_3 + MoO_3.$$

In the particular sample shown in Fig. 2b, about 26% of the starting molybdate has converted into $Nd_2(MoO_4)_3$ at 600 °C. Further in situ powder X-ray diffraction, with heating to 980 °C, did not reveal the formation of $Nd_6Mo_{10}O_{39}$.

$Nd_6Mo_{10}O_{39}$ is a therefore a non-equilibrium phase which presumably occurs along the pathway:

$$3Nd_2Mo_4O_{15} \rightarrow Nd_6Mo_{10}O_{39} + 2MoO_3$$
$$\rightarrow 3Nd_2(MoO_4)_3 + 3MoO_3.$$

3.2. Description of $Nd_6Mo_{10}O_{39}$ structure

Fig. 3 shows two projection views and a perspective drawing of the unit cell of $Nd_6Mo_{10}O_{39}$. Atomic coordinates and temperature factors are given in Table 2, and selected bond lengths in Table 3.

The structure of $Nd_6Mo_{10}O_{39}$ consists of seven and eight coordinate Nd atoms and MoO_4 tetrahedra. Two unique Nd atoms are eight coordinate. NdO_8 polyhedra share a face through three oxygen atoms, thus forming Nd_2O_{13}

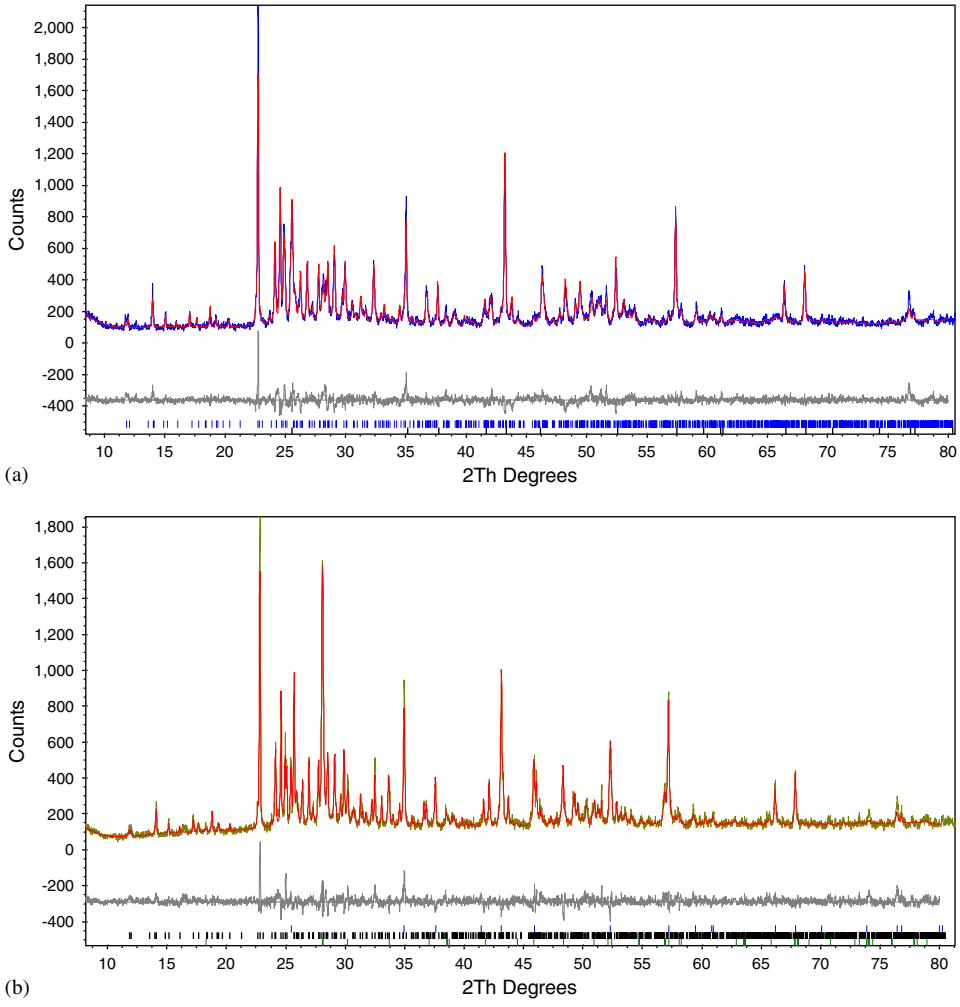

Fig. 2. Rietveld profiles (observed, calculated and difference) for decomposition of $Nd_2Mo_4O_{15}$: (a) 30 °C: $R_{wp} = 10.071\%$, the system contains $Nd_2Mo_4O_{15}$ and Al_2O_3 internal standard, (b) 600 °C, $R_{wp} = 10.111\%$, the system contains $Nd_2Mo_4O_{15}$, Al_2O_3 and $Nd_2(MoO_4)_3$.

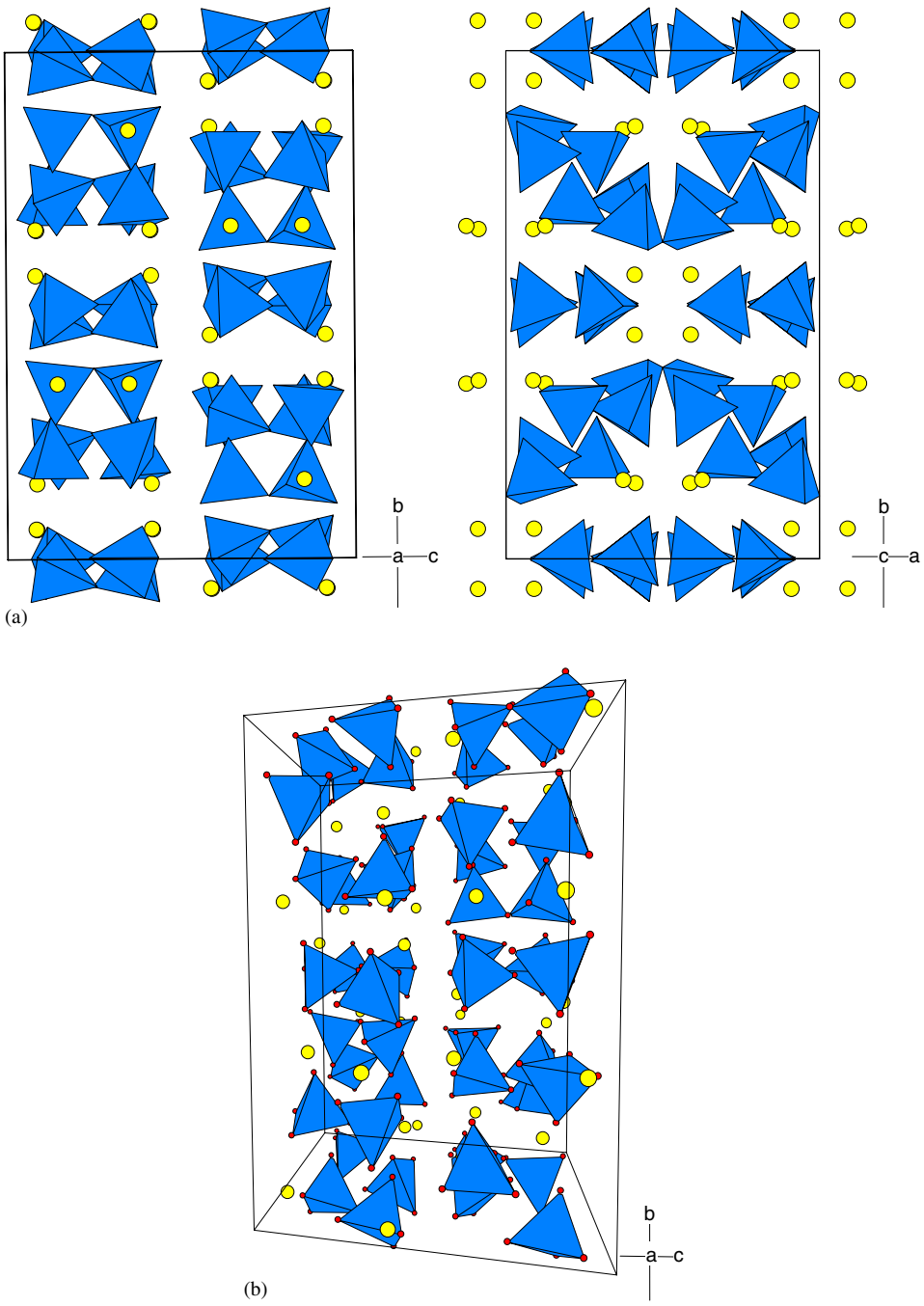

Fig. 3. (a) Two projection views of the crystal structure of $Nd_6Mo_{10}O_{39}$ at 120 K: dark polyhedra represent tetrahedral MoO_4 groups, light spheres are Nd atoms. (b) A perspective drawing: small circles at the corners of the dark tetrahedra represent O atoms. Positive directions of the three axes are indicated by axes labels.

units with a Nd(1)–Nd(2) distance of 3.7755(4) Å (Fig. 4a). The third unique Nd atom is seven coordinate and pairs of $Nd(3)O_7$ polyhedra share an edge, giving rise to Nd_2O_{12} units with a Nd(3)–Nd(3)′ distance of 3.7316(4) Å (Fig. 4b).

All five independent Mo atoms are found in a tetrahedral coordination environment. Four of these are isolated, regular MoO_4 groups, with Mo–O bond lengths ranging from 1.73 to 1.81 Å, and O–Mo–O bond angles from 105° to 115°. The remaining unique Mo atom is different, as its tetrahedra share a corner to form pyromolybdate $Mo(7)_2O_7$ groups (Fig. 5), with three shorter Mo–O distances of about 1.73 Å, a longer bond of 1.88 Å to the shared oxygen atom and a Mo(7)–O(14)–Mo(7) bridging angle of 143°. The geometry of the pyromolybdate group is virtually identical to that found in $Eu_6Mo_{10}O_{39}$. Bond valence calculations [18] give sums of 3.19, 3.35 and 3.38 for the three unique Nd atoms, and 5.89, 5.87, 6.09, 6.00 and 5.96 for the five unique Mo atoms, indicating that, on average, the Nd–O bonds are under compressive stress, while the Mo–O bonds are under tensile stress. One

Table 2
Fractional atomic coordinates and atomic displacement parameter isotropic equivalents for $Nd_6Mo_{10}O_{39}$

Atom	x	y	z	U_{eq} (Å^2)
Nd1	0.62608(1)	0.155268(9)	0.64678(1)	0.0047
Nd2	0.41289(1)	0.148771(9)	0.41431(1)	0.0048
Nd3	0.91044(1)	0.058904(9)	0.41602(1)	0.0057
Mo4	0.10326(2)	0.21643(1)	0.36184(2)	0.0052
Mo5	0.59452(2)	−0.02014(1)	0.36135(2)	0.0050
Mo6	0.18431(2)	−0.00059(1)	0.36069(2)	0.0055
Mo7	0.91358(2)	0.15382(1)	0.83909(2)	0.0070
Mo8	0.69320(2)	0.19286(1)	0.38136(2)	0.0063
O9	0.6072(2)	0.1706(1)	0.4682(2)	0.0077
O10	0.6087(2)	0.2516(1)	0.7426(2)	0.0093
O11	0.6040(2)	0.0543(1)	0.74340(2)	0.0096
O12	0.2390(2)	0.2016(1)	0.4192(2)	0.0100
O13	0.1260(2)	0.0025(1)	0.2350(2)	0.0118
O14	1.00	0.1235(2)	0.75	0.0105
O15	0.7285(2)	0.0048(1)	0.4146(2)	0.0103
O16	1.0783(2)	−0.0022(1)	0.9337(2)	0.0095
O17	0.2781(2)	0.0646(1)	0.3863(2)	0.0122
O18	0.9652(2)	0.1383(1)	1.1458(2)	0.0089
O19	0.7734(2)	0.1456(1)	0.7992(2)	0.0103
O20	0.7521(2)	0.0776(1)	0.6077(2)	0.0103
O21	0.7105(2)	0.2800(1)	0.3740(2)	0.0107
O22	0.4571(2)	0.0842(1)	0.5658(2)	0.0084
O23	0.4549(2)	0.22095(1)	0.5699(2)	0.0094
O24	0.9456(2)	0.2379(1)	0.8637(2)	0.0183
O25	0.5158(2)	0.0528(1)	0.3594(2)	0.0081
O26	0.9534(2)	0.1080(2)	0.9458(2)	0.0168
O27	0.6396(3)	0.1593(2)	0.2664(2)	0.0204
O28	0.8240(2)	0.1590(1)	0.4234(2)	0.0164

numerical indicator of the discrepancies between the bond valence sums found in a structure and the expected values is the global instability index, GII. Values of GII smaller than 0.05 v.u. correspond to structures with virtually no lattice-induced strain, while values of 0.20 v.u. and above suggests that the strain is sufficiently large for the structure to be unstable [19]. The calculated value of GII for $Nd_6Mo_{10}O_{39}$ is 0.15 and this might be related to the apparent metastable character of this phase. Similar behaviour is found in the RE_2MoO_6 family of rare-earth molybdates [20].

$Nd_6Mo_{10}O_{39}$ is isostructural with the analogous Eu compound, while $Ce_6Mo_{10}O_{39}$ has a slightly different, although closely related structure in space group P-1 [12,13]. The local coordination of Mo atoms in both structure types is the same: most of the tetrahedral MoO_4 groups are isolated, with one pair forming Mo_2O_7 groups. On the other hand, environments of the rare-earth cations differ. In $Ce_6Mo_{10}O_{39}$, there are six unique Ce atoms and they are all eight-coordinate. Two unique pairs of CeO_8 polyhedra share a face via three O atoms, forming Ce_2O_{13} units similar to those found in the title compound and the Eu analogue. A different CeO_8 pair share a face through four O atoms, giving rise to Ce_2O_{12} groups with a short Ce–Ce separation of 3.69 Å. The remaining CeO_8 pair share an edge, with the two central Ce atoms 4.16 Å apart.

Table 3
Selected bond lengths and bond valence sums for $Nd_6Mo_{10}O_{39}$

M	O	d (Å)	BVS (v.u.)
Nd1	O21	2.465(3)	3.19
	O9	2.465(2)	
	O10	2.362(2)	
	O11	2.461(3)	
	O19	2.533(2)	
	O20	2.333(3)	
	O22	2.605(2)	
	O23	2.553(3)	
Nd2	O27	2.480(3)	3.35
	O24	2.414(3)	
	O9	2.429(2)	
	O12	2.414(3)	
	O17	2.346(3)	
	O22	2.437(2)	
	O23	2.564(2)	
	O25	2.492(2)	
Nd3	O26	2.506(3)	3.38
	O18	2.471(2)	
	O16	2.395(3)	
	O13	2.346(3)	
	O16	2.342(2)	
	O15	2.499(3)	
	O28	2.272(3)	
Mo4	O23	1.795(2)	5.89
	O10	1.787(2)	
	O18	1.763(2)	
	O12	1.750(3)	
Mo5	O22	1.815(2)	5.87
	O11	1.789(2)	
	O15	1.762(3)	
	O25	1.745(2)	
Mo6	O16	1.807(3)	6.09
	O20	1.740(3)	
	O13	1.761(3)	
	O17	1.735(3)	
Mo7	O14	1.882(1)	5.96
	O19	1.734(3)	
	O24	1.737(3)	
	O26	1.730(3)	
Mo8	O9	1.809(2)	6.00
	O21	1.749(3)	
	O27	1.744(3)	
	O28	1.754(3)	

The existence of different, but related crystal structure types for $RE_6Mo_{10}O_{39}$ compounds is presumably related to the preference of the larger rare-earth cations such as Ce^{3+} for a higher average coordination number relative to the smaller RE^{3+} species. Similar instances of polymorphism in rare-earth molybdates can be found in the RE_2MoO_6 and $RE_2Mo_4O_{15}$ structural families [20,21].

4. Conclusions

An investigation of the Nd_2O_3–MoO_3 phase system has led to the isolation of a new neodymium molybdate,

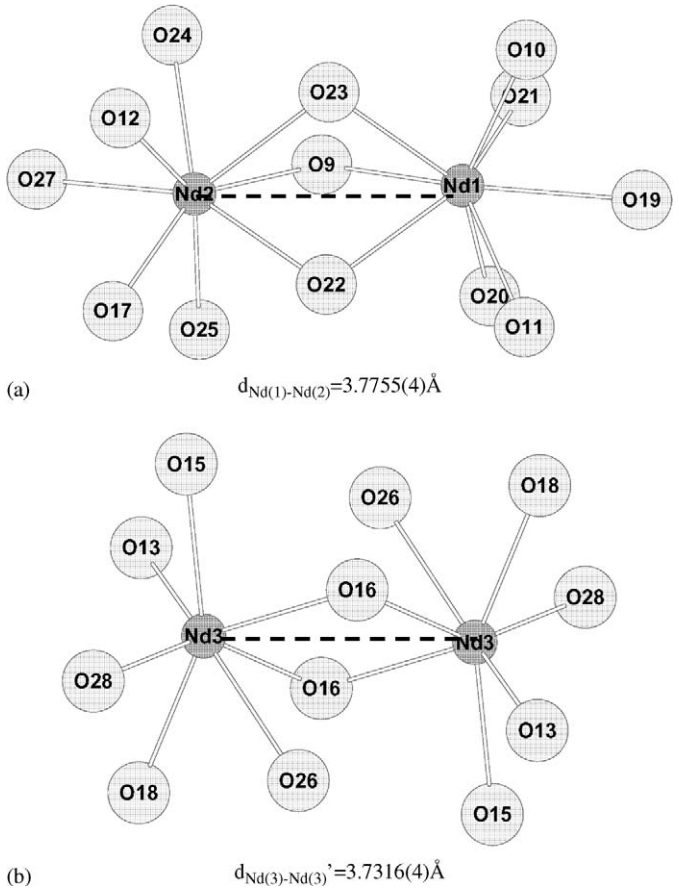

Fig. 4. Coordination environment of Nd atoms in $Nd_6Mo_{10}O_{39}$: (a) Nd_2O_{13} groups formed by face-sharing of two NdO_8 polyhedra; (b) Nd_2O_{12} groups formed by edge-sharing of two NdO_7 polyhedra.

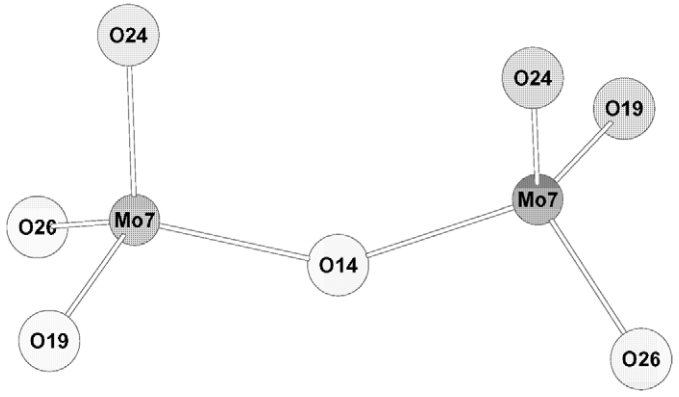

Fig. 5. A pyromolybdate group in $Nd_6Mo_{10}O_{39}$.

$Nd_6Mo_{10}O_{39}$, both in the form of single crystals and as a polycrystalline product. Variable temperature powder X-ray diffraction studies have shown that $Nd_6Mo_{10}O_{39}$ is a non-equilibrium phase, which can form on the pathway of decomposition of $Nd_2Mo_4O_{15}$ into $Nd_2(MoO_4)_3$. The successful isolation of the title phase depends critically on the precise heating regime used, as experiments with a number of different samples of $Nd_2Mo_4O_{15}$ have shown that it is possible to decompose it into $Nd_2(MoO_4)_3$ and continue slow-heating to the melting point without the formation of $Nd_6Mo_{10}O_{39}$.

The structure of $Nd_6Mo_{10}O_{39}$ has been determined by single crystal X-ray diffraction. It contains seven- and eight-coordinate Nd atoms, whose coordination polyhedra share edges and faces to form Nd_2O_{12} and Nd_2O_{13} groups. All Mo atoms are tetrahedral, with some of the MoO_4 tetrahedra sharing vertices to form Mo_2O_7 groups. $Nd_6Mo_{10}O_{39}$ is isostructural with $Eu_6Mo_{10}O_{39}$, and closely related to $Ce_6Mo_{10}O_{39}$.

Acknowledgments

RSB and IRE thank the Nuffield Foundation for the Undergraduate Research Bursary. IRE thanks the EPSRC for the Academic Fellowship. The authors would like to thank Judith Howard for the use of single crystal equipment and John Evans for powder diffraction facilities.

References

[1] D.D. Agarwal, K.L. Madhok, H.S. Goswami, React. Kinet. Catal. Lett. 2 (1994) 225.
[2] F. De Smet, M. Devillers, C. Poleunis, P. Bertrand, J. Chem. Soc. Faraday Trans. 94 (1998) 941.
[3] F. De Smet, P. Ruiz, B. Delmon, M. Devillers, J. Phys. Chem. B 105 (2001) 12355.
[4] A.W. Sleight, T.A. Mary, J.S.O. Evans, US Patent 5,919,720, 1999.
[5] W. Jeitschko, Acta Crystallogr. B 28 (1972) 60.
[6] S.C. Abrahams, C. Svensson, J.L. Bernstein, J. Chem. Phys. 72 (1980) 8,4278.
[7] P. Lacorre, F. Goutenoire, O. Bohnke, R. Retoux, Y. Laligant, Nature 404 (2000) 856.
[8] P. Gall, P. Gougeon, M. Greenblatt, W.H. McCarroll, K.V. Ramanujachary, J. Solid State Chem. 134 (1997) 45.
[9] K.V. Ramanujachary, M. Greenblatt, W.H. McCarroll, J.B. Goodenough, Mater. Res. Bull. 28 (1993) 1257.
[10] P. Gall, H. Noël, P. Gougeon, Mater. Res. Bull. 28 (1993) 1225.
[11] ICSD, Fachinformationszentrum (FIZ), Karlsruhe, 2005.
[12] B.M. Gatehouse, R. Same, J. Solid State Chem. 25 (1978) 115.
[13] H. Naruke, T. Yamase, J. Solid State Chem. 161 (2001) 85.
[14] SAINT+, Release 6.22. Bruker Analytical Systems, Madison, Wisconsin, USA, 1997–2001.
[15] G.M. Sheldrick, SADABS, University of Göttingen, Germany, 1998.
[16] A. Altomare, G. Cascarano, C. Giacovazzo, A. Guagliardi, M.C. Burla, G. Polidori, M. Camalli, J. Appl. Crystallogr. 27 (1994) 435.
[17] P.W. Betteridge, J.R. Carruthers, R.I. Cooper, K. Prout, D.J. Watkin, J. Appl. Crystallogr. 36 (2003) 1487.
[18] I.D. Brown, D. Altermatt, Acta Crystallogr. B 41 (1985) 244.
[19] I.D. Brown, Zeit. Kristall. 199 (1992) 255.
[20] J.A. Alonso, F. Rivillas, M.J. Martinez-Lope, V. Pomjakushin, J. Solid State Chem. 177 (2004) 2470.
[21] H. Naruke, T. Yamase, J. Solid State Chem. 173 (2003) 407.